Environ. Eng. Res. Vol. 11, No. 5, pp. 241~249, 2006
Korean Society of Environmental Engineers

HYSTERETIC MODELING ON THE CONVECTIVE TRANSPORT OF ORGANIC SOLVENT IN AN UNSATURATED SOIL ZONE

Kun Sang Lee

Department of Environmental Engineering
Kyonggi University, Suwon, Kyonggi 443-760, S. Korea

Abstract : A mathematical model is described for the prediction of convective upward transport of an organic solvent driven by evaporation at the surface, which is known as the major transport mechanism in the *in-situ* photolysis of a soil contaminated with 2,3,7,8-tetrachlorodibenzo-p-dioxin(TCDD). A finite-element model was proposed to incorporate the effects of multiphase flow on the distribution of each fluid, gravity as a driving force, and the use of hysteretic models for more accurate description of *k-S-p* relations. Extensive numerical calculations were performed to study fluid flow through three types of soils under different water table conditions. Predictions of relative permeability-saturation-pressure (*k-S-p*) relations and fluids distribution for an illustrative soil indicate that hysteresis effects may be quite substantial. This result emphasizes the need to use hysteretic models in performing flow simulations including reversals of flow paths. Results of additional calculations accounting for hysteresis on the one-dimensional unsaturated soil columns show that gravity affects significantly on the flow of each fluid during gravity drainage, solvent injection, and evaporation, especially for highly permeable soils. The rate and duration of solvent injection also have a profound influence on the fluid saturation profile and the amount of evaporated solvent. Key factors influencing water drainage and solvent evaporation in soils also include hydraulic conductivity and water table configuration.

Key Words : 2,3,7,8-tetrachlorodibenzo-p-dioxin(TCDD), Multiphase flow, Hysteresis, Mathematical model

INTRODUCTION

The contamination of soil with 2,3,7,8 -tetrachlorodibenzo-p-dioxin(TCDD) has become a matter of major concern recent years. TCDD has extremely low water solubility and volatility and thus can be very persistent once introduced into the soil environment.[1] Other chemicals such as polychlorinated biphenyls(PCBs) and chlorinated furans exhibit a similar behavior. Pyrolysis and chemical treatment have been proposed as means of soil decontamination. Being very effective, both of these methods can also prove to be expensive.

Recently, 2,3,7,8-TCDD was found to photo-degrade rapidly under the proper conditions although generally a very stable molecule. In order for this to occur, the TCDD must be dissolved in a light-transmitting film, in the presence of an organic hydrogen donor, under ultraviolet light. This discovery led to the possibility of spraying the soil surface with some low-toxicity organic solvents and allowing sunlight to photodegrade the TCDD.

The proposed technology of *in-situ* soil decontamination involves the addition of an organic solvent to the soil to remove the tightly-bound TCDD and effect the movement to the soil surface with subsequent decomposition

† Corresponding author
E-Mail: kslee@kyonggi.ac.kr
Tel: 82-31-249-9738, Fax: 82-31-244-6300

by ultraviolet light. This process would be desirable because it would cost relatively low and be implemented easily. It would also avoid the risk of the storage or transport of TCDD -contaminated soil, and it would not be destructive to the site.

Previous research has shown that a convective upward movement of TCDD with evaporating solvents was found to be the major transport mechanism. Dougherty *et al.*[2] performed experimental and numerical studies on the migration of solvent through uniform soils. A series of wind tunnel tests with uniform or simple nonuniform media were carried out to investigate effects of soil particles on the evaporation in soil.[3,4] To investigate the effects of physicochemical characteristics of nonuniform soils on the transport of water or solvent through an unsaturated zone, Lee[5,6] developed a convective transport model incorporating Brooks -Corey equation. Most of previous studies, however, derived conclusions based on the experimental results under limited ranges of parameters or idealized laboratory conditions. Yang and Yanful[7] used experimental measurements and analytical methods to study upward and downward water fluxes through different soils. To understand and predict the actual migration of solvent and saturation profile more effectively, it is necessary to have a more accurate mechanistic description and numerical model on the solvent transport in the soil.

The objective of this study is to investigate some of important factors that affect the convective transport of an organic solvent in the unsaturated soils under different water table conditions. In order to accomplish this objective, a finite-element-based numerical model was developed using three-phase flow equations in conjunction with hysteretic relative permeability -saturation-pressure(k-S-p) relationships.

MATHEMATICAL FORMULATION

A theoretical analysis on the liquid flow through an unsaturated soil zone involves deriving and solving a partial differential equation describing the liquid velocity and saturation in the nonuniform soil column. Writing this equation in a manageable form, one overcomes limited applicabilities of earlier models by removing some of simplifications made in previous studies.

Dougherty *et al.*[2] assumed that the fluid behavior in the soil can be adequately represented by including only two fluid phases in the model. When a solvent is applied to partially-saturated soil, there are actually three phases, a gas phase, an aqueous phase, and an organic solvent phase. To represent the fluid saturation more accurately, the model, therefore, includes three phases. The fluid wettability is constrained to follow water-solvent-gas, from most to least. Capillary pressure and relative permeability as functions of fluid saturations are estimated using van Genutchen[8]'s equations. The effect of gravity in the soil environment can also contribute to the convective flow and is taken into account.

Continuity Equation

With these assumptions, the mass balance for fluid phase can be written as follows:[9]

$$\frac{\partial(nS_\alpha)}{\partial t} + \nabla \cdot (nS_\alpha \mathbf{v}_\alpha) = 0 \qquad (1)$$

where n is the porosity, S_α is saturation of the α-phase, $\mathbf{v}_\alpha$ is the average velocity of the α -phase[LT^{-1}]. As stated earlier, three phases including water(w), gas(g), and solvent(n) are considered.

Phase velocity defined in Eq. (1) is written in terms of the multiphase extension of Darcy's law.

$$\mathbf{v}_\alpha = -\frac{\mathbf{k}k_{r\alpha}}{nS_\alpha\mu_\alpha} \cdot (\nabla p_\alpha - \gamma_\alpha \nabla z) \qquad (2)$$

where p_α is the α-phase pressure[$ML^{-1}T^{-2}$], μ_α is the α-phase viscosity[$ML^{-1}T^{-1}$], $\mathbf{k}$ is the intrinsic permeability tensor[L^2], and $k_{r\alpha}$ is the relative permeability. Effects of gravity is included in the specific gravity($\gamma_g = \rho_\alpha g$).

Equations (1) and (2) are combined into the following governing equation amendable to solution by a standard finite-element method.

$$\frac{\partial(nS_\alpha)}{\partial t}+\nabla\cdot\left[-\frac{\mathbf{k}k_{r\alpha}}{\mu_\alpha}\cdot(\nabla p_\alpha-\gamma_\alpha\nabla z)\right]=0 \qquad (3)$$

Hydraulic Properties

The use of Eq. (3) requires knowledge of two soil hydraulic functions: capillary pressure curve $p_{c\alpha_1\alpha_2}(S_{\alpha_2})$, and relative permeability function $k_{r\alpha}(S_\alpha)$. In this study, a representation of hydraulic properties is based on a combination of hysteretic van Genutchen's *k-S-p* model and Mualem[10]'s equation.

By modifying van Genutchen's *k-S-p* equation, a hysteretic saturation-pressure function is written as

$$p_c=\frac{\rho_w g}{a}\left(S_e^{-\frac{1}{m}}-1\right)^{\frac{1}{\eta}} \qquad (4)$$

where p_c is the capillary pressure[$ML^{-1}T^{-2}$], ρ is the density[ML^{-3}], S_e is the effective saturation, a is the scaling factor[L^{-1}], η is the curve-fitting parameter, and $m=1-\frac{1}{\eta}$. p_c, S_e, and a are the flow-path, history-dependent parameters and are resulted from hysteresis.

Combination of (4) with Mualem's statistical model leads to the following expression for relative permeabilities k_{rw}, k_{rg}, and k_{rn} in terms of effective saturation $S_{e\alpha}$ and trapped saturation $S_{\alpha t}$.

$$k_{rw}(S_w)=S_{ew}^{\zeta}\left[\left(1-S_{wt}^{\frac{1}{m}}\right)^m-\left(1-S_w^{\frac{1}{m}}\right)^m\right] \qquad (5)$$

$$k_{rg}=S_{eg}^{\phi}\left\{\left[1-\left(1-S_g\right)^{\frac{1}{m}}\right]^m-\left[1-\left(1-S_{gt}\right)^{\frac{1}{m}}\right]^m\right\} \qquad (6)$$

$$k_{rN}=S_{eN}^{\xi}\left\{\left[1-\left(S_w+S_{Nwt}\right)^{\frac{1}{m}}\right]^m-\left[1-\left(1-S_g-S_{Nnt}\right)^{\frac{1}{m}}\right]^m\right\} \qquad (7)$$

where ζ, ϕ, and ξ are pore connecting parameters for water, gas, and solvent, and are assumed as 0.5.[11] These equations include hysteresis as the result of fluid entrapment effects through $S_{e\alpha}$ and $S_{\alpha t}$.

Initial and Boundary Conditions

The flow equation (3) can be solved with proper initial and boundary conditions. The initial condition used for the solution of the equation is that the soil zone is saturated with water at the start of the test.

$$S_w(x,0)=1.0 \qquad (8)$$

The water level is kept constant, leading to a prescribed water head assigning at the bottom of the soil column. This value is determined from the level of water table.

$$h_w(l,t)=h_{wo} \qquad (9)$$

At the top of the column, three combinations of boundary conditions are consecutively applied. Atmospheric gas pressure was assigned during gravity drainage stage. Then, constant injection rate of solvent and atmospheric gas pressure are used. During evaporation stage, fluid distribution is not known. Allocation of evaporation rate to each fluid is based on fractional flow. Given that total flow rate is set to v_t[LT^{-1}], the phase flux is defined as:

$$v_\alpha=f_\alpha v_t \qquad (10)$$

where f_α is the fractional flow defined by phase mobilities $\lambda_\alpha=\frac{kk_{r\alpha}}{\mu_\alpha}$ [$M^{-1}LT$].

$$f_\alpha=\frac{\lambda_\alpha}{\lambda_w+\lambda_n+\lambda_g} \qquad (11)$$

SIMULATION RESULTS

Simulation Scenarios

To understand the physical process involved in the convective transport, a theoretical analysis was undertaken. Because the flow equation is dependent on *k-S-p* relationship and highly

nonlinear, solutions are obtained with the finite-element program used by Lee[12]. A 2.0 m long soil column was used to calculate drainage and evaporation from the column under specified water table levels. The water table position ranges from −130 cm to −170 cm depth.

The hypothetical scenario involves sequence of three stages or events to represent a physical situation during the sunlight exposure experiment. In the first stage, referred to as the initial gravity drainage, the initially water-saturated soil is allowed to drain, therefore creating a static saturation profile. In the second and third stages, called solvent injection and evaporation stages, respectively, the soil column is treated with an organic solvent at the top surface and then exposed to evaporation for 5 hours. In the numerical model, the top layer of grids is assigned to be a source into which the model adds the designated volume of solvent over injection period, or a sink from which it removes the designated total volume of fluids over evaporation period.

Duration of each period, injection rate of solvent, and total evaporation rate were determined according to the results of preliminary simulations. As proposed by Dougherty *et al.*[2], the applied solvent is tetradecane($C_{14}H_{30}$). Table 1 gives the relevant physical and chemical properties of tetradecane taken from Lide[13].

Calculations were carried out for three types of soils including sand, loam, and silt. The hydraulic properties(n, S_{wr}, S_{gr}, and k) and van Genutchen parameters(a_i, a_d and η) of the soils are listed in Table 2, originally obtained by Carsel and Parrish[14]. Table 3 summarizes duration of each flow period and boundary conditions for sand, loam, and silt.

Table 1. Physical properties of fluids used in the simulations

	water	gas	tetradecane
viscosity (poise)	0.01	0.0002	0.021
density (g/cm^3)	0.9982	0.00129	0.763
surface tension (dyne/cm)	σ_{gw} = 72.75, σ_{nw} = 37.3, σ_{gn} = 26.56		

Simulation Analysis

As an illustrative example, one presents detailed results for loam. Figures. 1(a), (b), (c) and (d) display the calculated hydraulic properties of this soil for four different displacement processes such as primary imbibition curve(PIC), primary drainage curve(PDC), main imbibition curve(MIC), and main drainage curve(MDC). A comparison of the curves shows that there are insignificant differences among $k_{rw}(S_w)$ and $k_{rg}(S_L)$ curves and the large differences among $p_{cnw}(S_w)$ and $p_{cgn}(S_L)$ curves over entire range of saturation values, where S_L is total wetting phase saturation relative to the gas phase, that is $S_L = S_w + S_n$. From these results, it is predicted that simulations without consideration on hysteresis may produce highly unacceptable results for the cases including reversals of flow paths.

Two numerical simulations were conducted to evaluate the significance of hysteresis on fluid distribution at the end of major periods. One considers a 2.0 m long loam column with an

Table 2. Hydraulic properties of soils used in the simulations

	n	S_{wr} [1]	S_{gr} [2]	a_d [3] (cm^{-1})	a_i [4] (cm^{-1})	η [5]	k (cm$_2$)
sand	0.43	0.105	0.1	0.145	0.152	2.68	8.42×10^{-6}
loam	0.43	0.181	0.1	0.036	0.040	1.56	2.95×10^{-7}
silt	0.46	0.074	0.1	0.016	0.017	1.37	7.09×10^{-8}

1) residual water saturation
2) residual gas saturation
3) scaling parameter for drainage in van Genutchen equation [L^{-1}]
4) scaling parameter for imbibition in van Genutchen equation [L^{-1}]
5) curve-fitting shape parameter for van Genutchen equation

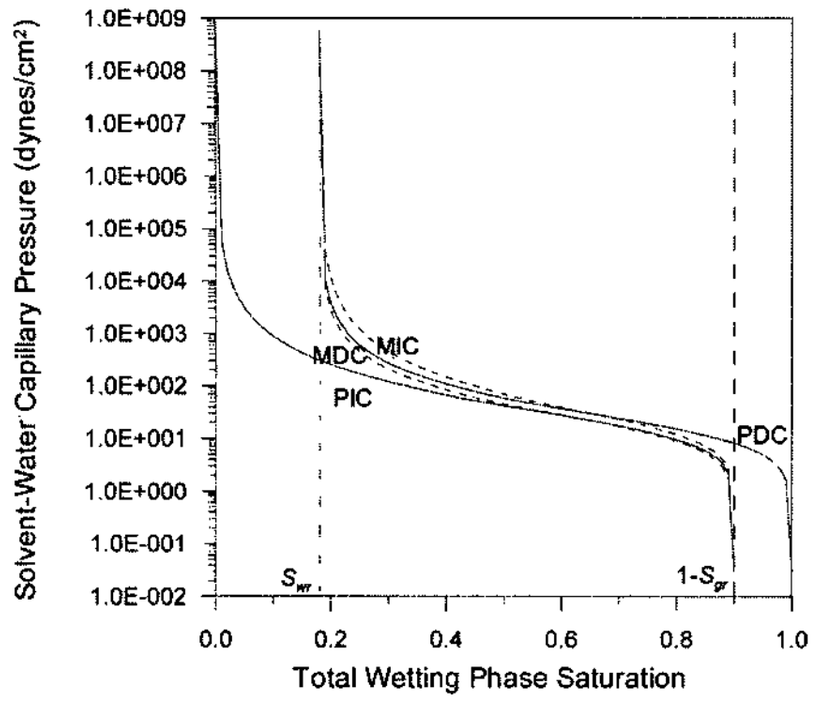

(a) solvent-water capillary pressure

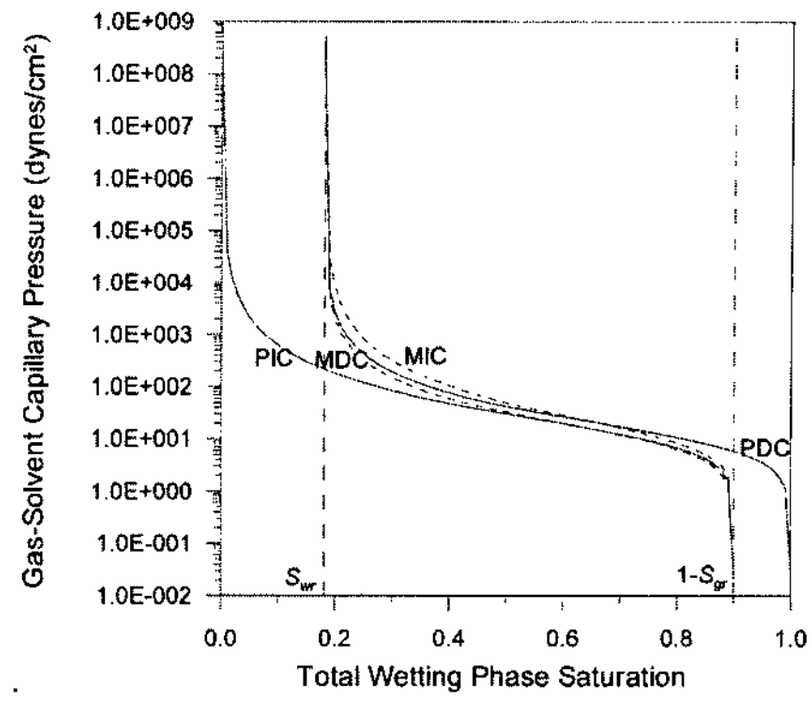

(b) gas-solvent capillary pressure

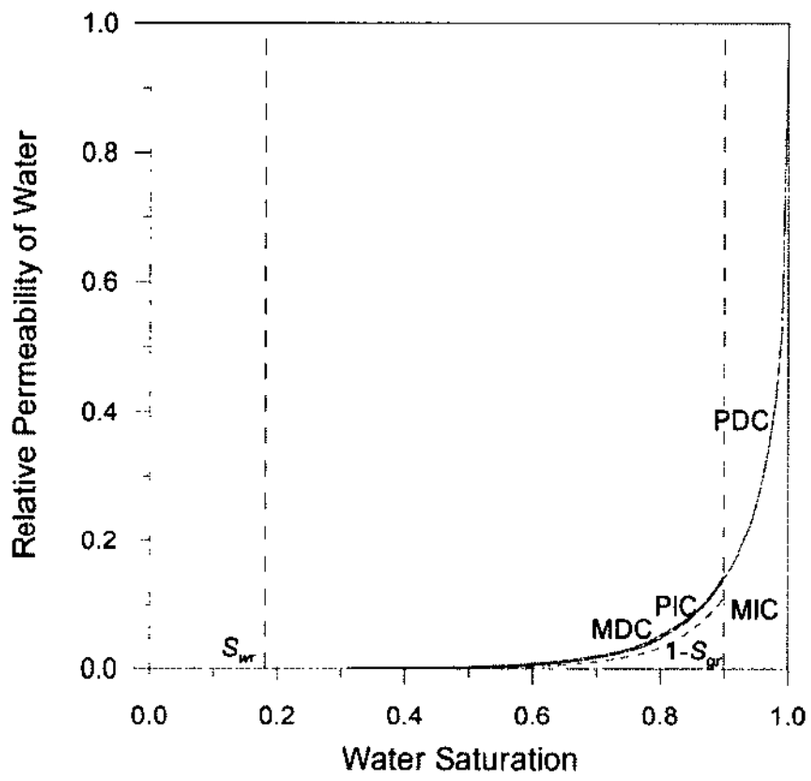

(c) relative permeability of water

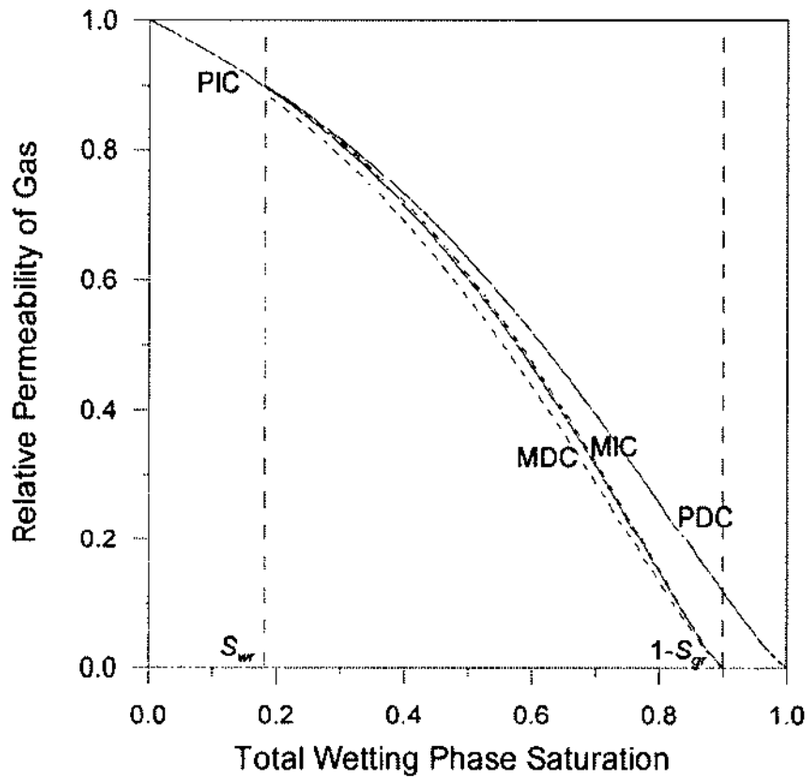

(d) relative permeability of gas

Figure 1. Hysteretic relationship among relative permeability, saturation, and capillary pressure for loam.

imposed water head of 60 cm at the bottom of column(level of water table = −140 cm), assuming solvent injection rate of 5×10^{-4} $cm^3/cm^2/sec$ and evaporation of 0.75 $cm^3/cm^2/sec$. Durations of gravity drainage, constant flux injection of solvent, and evaporation periods are 4 hr, 2.5 hr, and 5 hr, respectively. The fluid saturation in the soil column after each period were simulated.

As the gravity drainage process proceeds, fluid distribution reaches an equilibrium with water saturation decreasing at the top part of the soil column[Figure 2(a)]. When downward infiltration of an organic solvent with a constant flux condition is simulated, the gas saturation decreases as the top part of the column fills with solvent[Figure 2(b)]. During an evaporation period, both upward flux due to evaporation and downward flux due to gravity are simultaneously occurred[Figure 2(c)]. At the surface,

Table 3. Boundary conditions and their duration during major steps in the simulations

	gravity drainage			solvent injection			evaporation		
	boundary conditions		duration (hr)	boundary conditions		duration (hr)	boundary conditions		duration (hr)
	surface	bottom		surface	bottom		surface	bottom	
sand	$p_g = p_{atm}$	$h_w = h_{wo}$	1	$p_g = p_{atm}$ $v_n = v_{no}$	$h_w = h_{wo}$	0.16-1	$p_g = p_{atm}$ $v_t = v_{to}$	$h_w = h_{wo}$	5
loam			4			2.5-5			5
silt			10			2.5-5			5

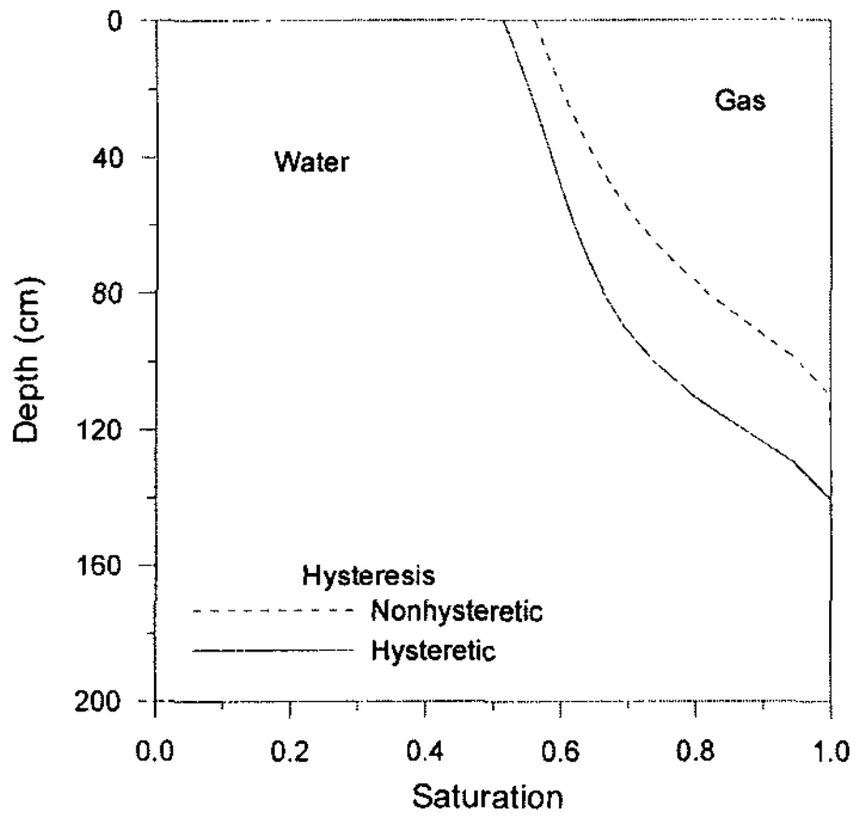

(a) after gravity drainage

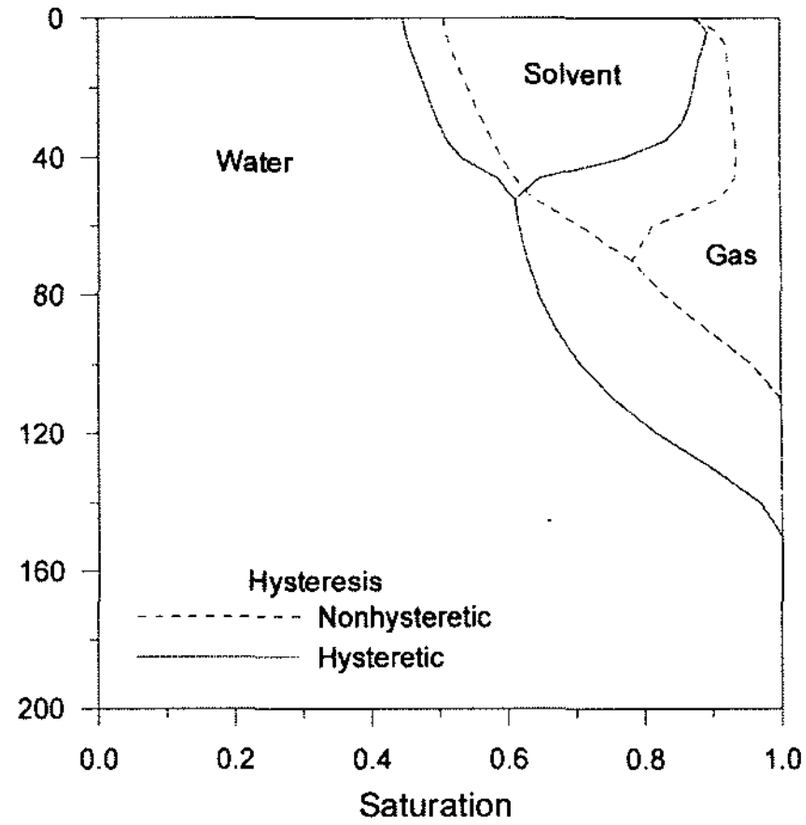

(b) after solvent injection

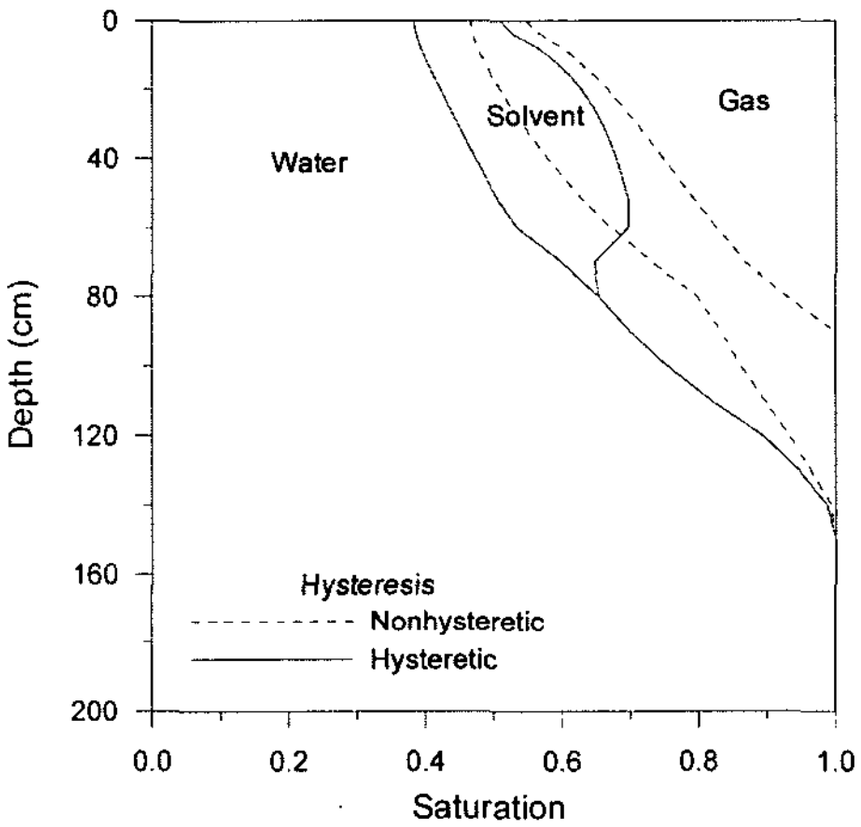

(c) after evaporation

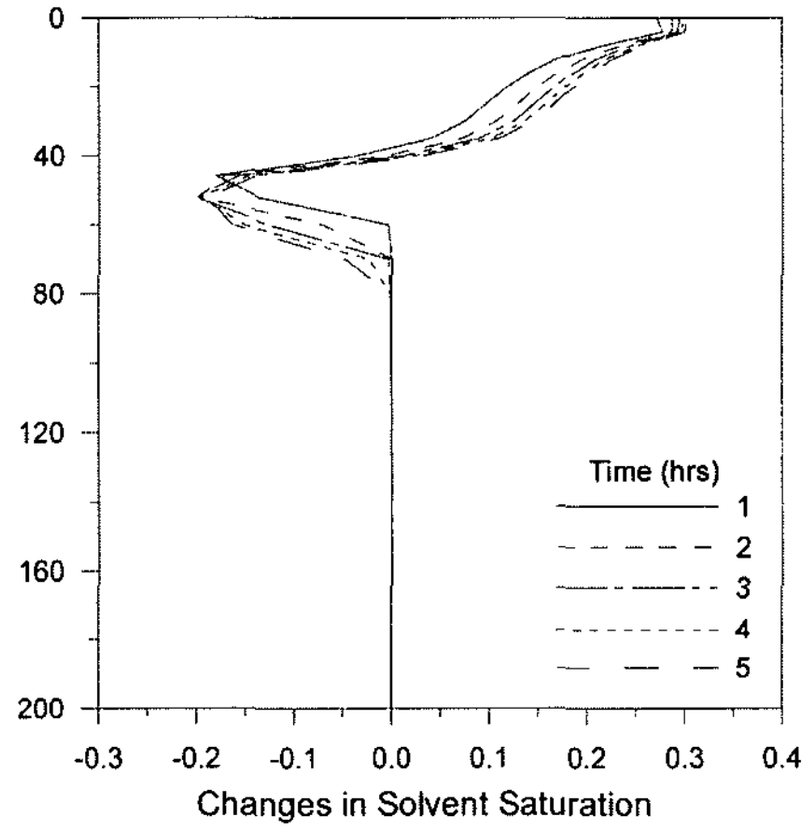

(d) changes in solvent saturation during evaporation

Figure 2. Saturation profiles of fluids during major steps for loam (water table = −140 cm, V_{no} = 5×10^{-4} $cm^3/cm^2/sec$, V_{no} = 0.75 $cm^3/cm^2/sec$).

solvent saturation decreases quickly to the level of residual saturation.

Figures 2(a), (b), and (c) compare results with the nonhysteretic hydraulic properties(dashed lines) with calculations from the hysteretic model(solid lines). Comparison of saturation profiles indicates a distinct difference in results between two models. Differences in the distributions of fluid saturation can reach more than 100% for depths occurring reversals of flow paths. This result indicates an urgent need for the use of hysteretic models to perform more reliable simulations.

During the evaporation stage, the solvent saturation was calculated hourly to obtain the amount of solvent changed by evaporation and drainage. The data in Figure 2(d) with hysteretic models indicates a solvent evaporation that shows a rapid decrease within two hours, followed by remaining almost constant. The negative values below 40 cm indicate that the solvent saturation was increased by downward flux due to gravity.

A serious of calculations were also conducted to assess the relative importance of the effects of solvent injection rate and total evaporation rate on the amount of evaporated solvent in different soils. Simulations were carried out for

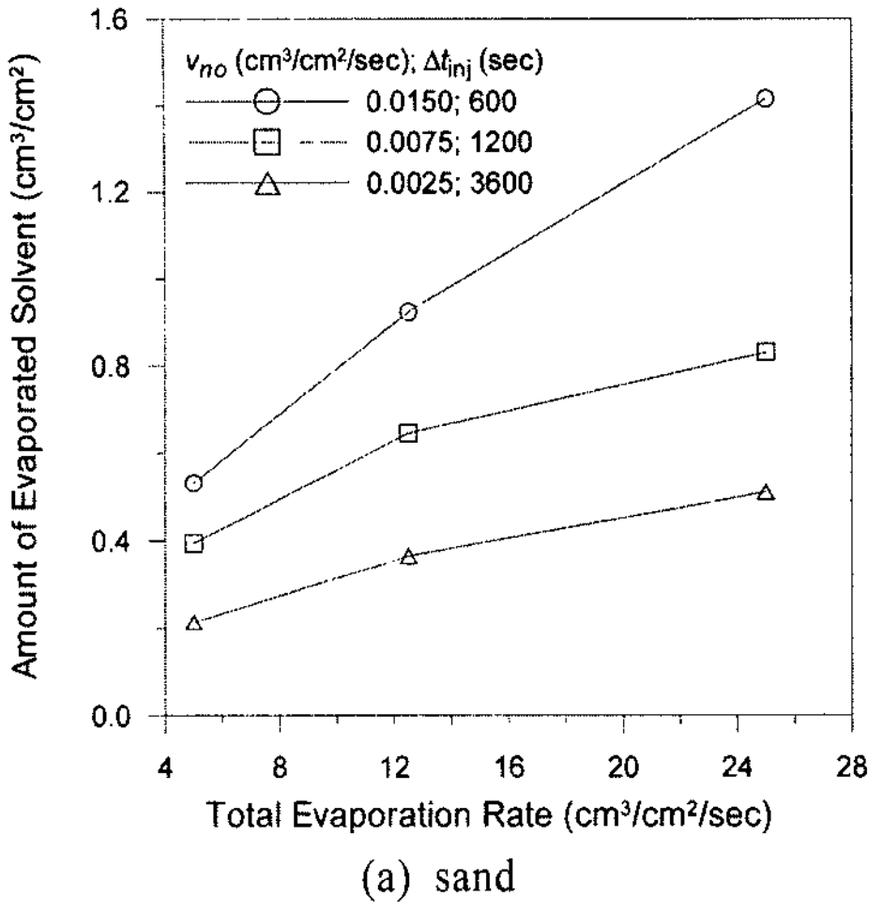

(a) sand

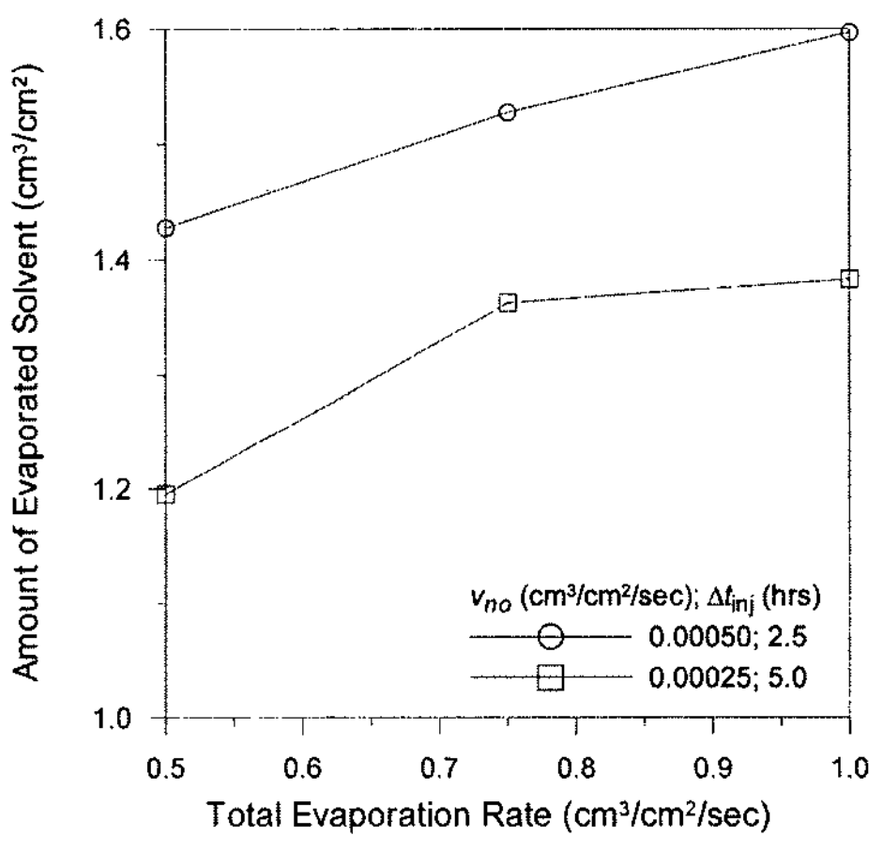

(b) loam

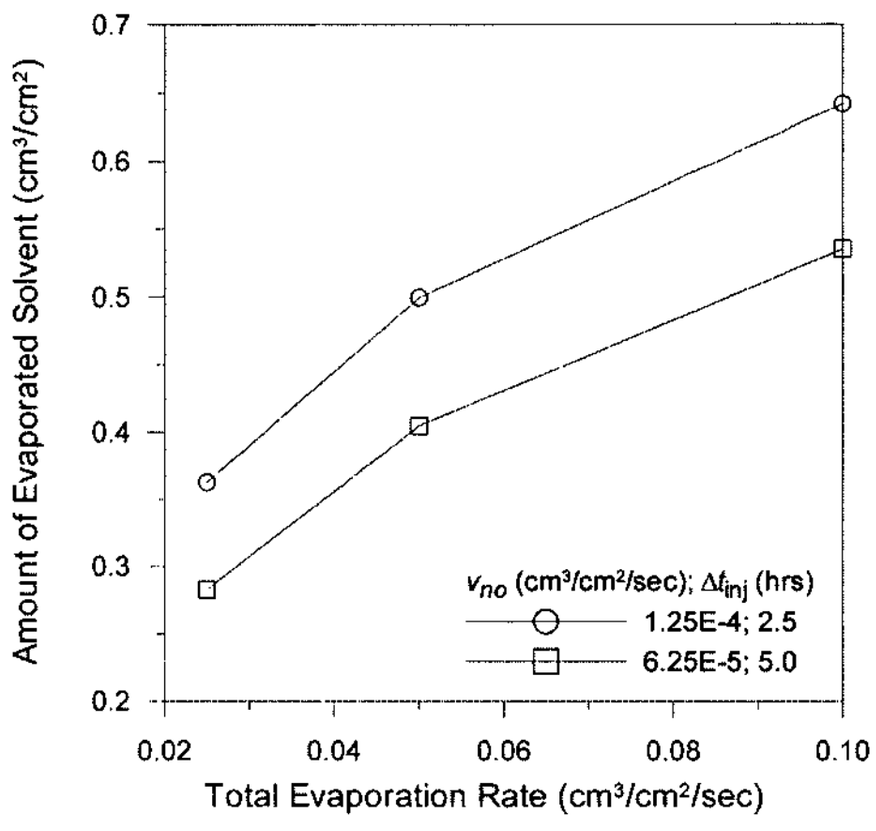

(c) silt

Figure 3. Amount of evaporated solvent for different soil textures, solvent injection rates and time, and total evaporation rates(water table = −110 cm).

all soil types listed in Table 3 with hysteretic models. The amounts of evaporated solvent per unit area from the surface were calculated from the difference in solvent saturation before and after evaporation. It is assumed that the level of water table is −110 cm and amount of total injection is fixed for each soil. The results in Figure 3. indicate that higher rate of injection during shorter period results in increased amount of evaporated solvent for all cases considered. The differences are a consequence of decreased downward flux due to gravity for the case of high injection rate. In addition, increased total evaporation rate results in an increased amount of evaporation.

The effects of the level of water table on the amount of evaporation were further analyzed. Calculations were performed for water table levels of −110 cm, −140 cm, and −170 cm. Operation method for each period is summarized in Table 4.

Table 4. Rate and duration during solvent injection and evaporation periods

	solvent injection		evaporation	
	rate ($cm^3/cm^2/sec$)	duration (hr)	rate ($cm^3/cm^2/sec$)	duration (hr)
sand	0.0125	0.33	12.5	5
loam	5×10^{-4}	2.5	0.75	5
silt	6.25×10^{-5}	5.0	0.05	5

Figure 4. shows that deepening water table elevation increases evaporation in all soil columns. Deepening water table elevation promotes the gravity-driven drainage, especially for coarse -textured soil, hence solvent supply to the soil surface increased. Increased saturation of solvent at the top results in higher mobility and increased evaporation. The relative importance of the effects of soil textures on evaporation was assessed by further analyzing Figure 4. Deepening water table elevation increases evaporation in sands and to much lesser extent in the finer-textured soils. Differences associated with soil textures are a direct consequence of lesser gravity-driven drainage and higher water

saturation at the top for finer-textured soils, which do not allow enough solvent to be transported to the surface.

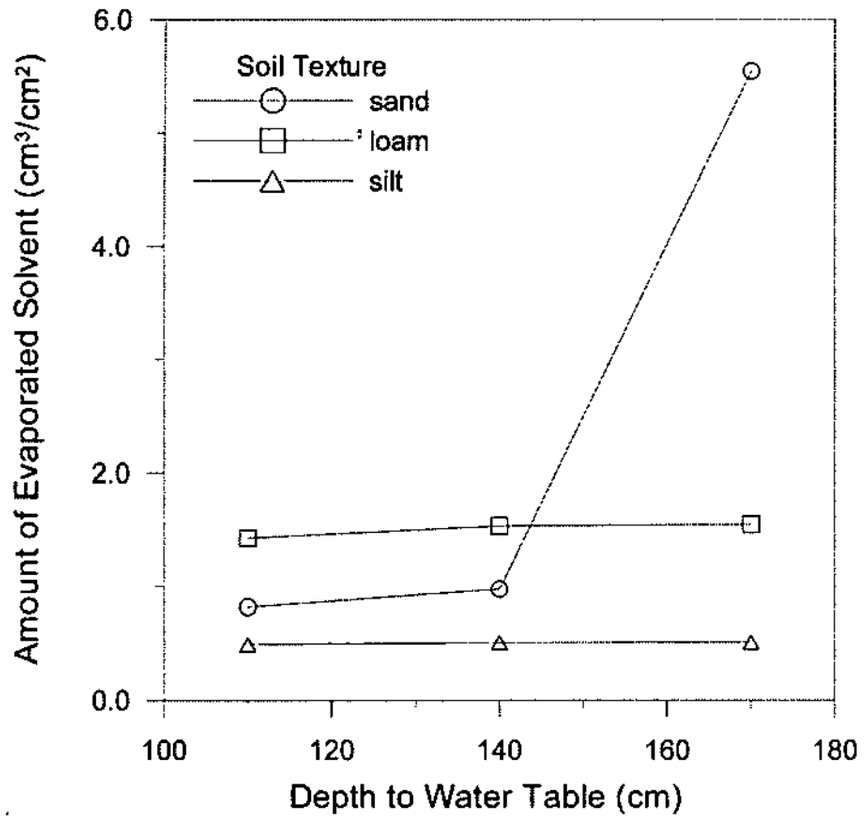

Figure 4. Amount of evaporated solvent for different soil textures and depth to water table.

CONCLUSIONS

The paper presents a three-phase flow model to predict the convective transport of tetradecane through unsaturated soils under different water table conditions. The mathematical formulation is obtained by using van Genutchen's *k-S-p* equation with hysteresis models in conjunction with Darcy's law including gravity. Use of a finite-element model allows one to analyze effects of soil types, solvent injection rate and time at the surface, total evaporation rate, and water table location on the fluid flow during major periods in the decomposition processes.

Calculations for loam show that the introduction of hysteresis may lead to significant differences in the *k-S-p* relationship. Considerable differences in the fluid saturation profiles were also obtained in the simulation of evaporation. Most of a solvent evaporation occurs within 40 cm depth in two hours.

A series of simulations with hystersis models were carried out to investigate factors affecting evaporation. Higher rate of injection during smaller time and increased total evaporation rate result in increased amount of evaporation. Deepening water table elevation increases evaporation in all soil columns due to promoted the gravity drainage and increased solvent supply to the soil surface. Under deepening water table conditions, evaporation is increased considerably in a coarse-textured soil and to much lesser extent in the finer-textured soils.

REFERENCES

1. LaGrega, M. D., Buckingham, P. L., and Evans, J. C., *Hazardous Waste Management*, 2nd Ed., McGraw-Hill, Boston (2001).
2. Dougherty, E. J., McPeters A. L., Overcast M. R., and Carbonell R. G., "Theoretical analysis of a method forin situ decontamination of soil Containing 2,3,7,8-tetrachlorodibenzo-p -dioxin," *Environ. Sci. Tech.*, **27**, 505-515 (1993).
3. Lee, S.-D. and Chung, I.-H., "Study on evaporation from the soil affected by the particle size and soil water content," *J. Kor. Soc. of Env. Eng.*, **19**(1), 1-8 (1997).
4. Lee, S.-D., Park, S.-C., and Lee, K.-I., "A study on the latent heat exchange model between soil and atmosphere," *J. Kor. Soc. of Env. Eng.*, **20**(11), 1511-1522 (1998).
5. Lee, K. S., "Finite-element simulation on the water migration through a nonuniform unsaturated zone," *Computer Methods and Advances in Geomechanics, Desai et al.* (eds), 837 -842 (2001).
6. Lee, K. S., "Finite-element modeling on the convective transport of an organic solvent through nonuniform soils during in-situ photolysis process," *Environ. Eng. Res.*, **8**(3), 122-129 (2003).
7. Yang, M. and Yanful, E. K., "Water balance during evaporation and drainage in cover soils under different water table conditions," *Adv. in Water Resourses,* **24**, 505-521 (2002).
8. van Genutchen, M. Th., "A closed-form equation for predicting the hydraulic conductivity of unsaturated soils," *Soil Sci. Soc. Am. J.*, pp. 892-898 (1980).
9. Helmig, R., *Multiphase Flow and Transport*

Processes in the Subsurface, Springer, Berlin, Germany, 47-82 (1997).
10. Mualem, Y., "A new model for predicting the hydraulic conductivity of unsaturated porous media", *Water Resources Res.,* **12**(3), 513-522 (1976).
11. Vogel, T., van Genuchten M. Th., and Cislerova, M., "Effect of the shape of the soil hydraulic functions near saturation on variably-saturated predictions," *Adv. in Water Resourses,* **24**, 133-144 (2001).
12. Lee, K.S., "Effects of hysteresis in hydraulic properties on the water flow through an unsaturated zone," *J. Kor. Soc. of Geosys. Eng.,* **41**(3), 187-193 (2004).
13. Lide, D. R., *CRC Handbook of Chemistry and Physics,* 83rd Edition, CRC Press, Boca Raton (2002).
14. Carsel, R. F. and Parrish, R. S., "Developing joint probability distributions of soil water retention characteristics," *Water Resources Res.,* **24**(5), 755-769 (1988).